osteoblast differentiation. In contrast, Hivep3 increased not only the level of *Creb3l2*, but also of other canonical ER stress-related genes in ATDC5 chondrocytes, although loss of *Alg2* decreased the expression of *Creb3l2*. These results suggest that the Hivep3-Alg2 pathway is important for physiological ER stress in chondrocytes.

Although Hivep2 and Hivep3 showed cooperative roles in decreasing bone formation and bone volume *in vivo* (17), Saita *et al.* (16) reported results similar to ours where gain of Hivep2 expression enhanced osteoblast differentiation, and Hivep2 knock-out osteoblasts failed to support efficient osteoclastogenesis *in vitro*. In addition, they showed that bone formation, as well as bone resorption, decreased in the bones of Hivep2-null mice, resulting in osteopenia due to the low turnover of bone remodeling. Recently, Hivep3 was also found to promote osteoclastogenesis (14, 15). Taken together, the defects in osteoclastogenesis induced by loss of the Hivep genes seem to be mainly responsible for the additively increased bone volume in *Hivep2*/*Hivep3* double knock-out mice. In contrast, we showed that each of the three Hivep genes was essential for chondrogenesis *in vitro*, suggesting that the chondrodysplasia observed following combined ablation of Hivep2 and Hivep3 in mice (17) was a result of the loss of the cell autonomous action of the Hivep proteins. Although we found the physiological ER stress and the level of *Creb3l2* to be increased by the Hivep3-Alg2 axis, the precise molecular mechanisms are unclear. Moreover, it is still unclear why the three Hivep genes exhibit diverse actions in osteogenesis. Because expression of *Alg2* was not altered by loss of Hivep1 or Hivep2, other molecular targets downstream of Hivep1 or Hivep2 should be evaluated. Although Hivep proteins are known to act as transcription factors as well as scaffolds, they may harbor some other unknown properties, as most of the area of the large proteins has not been classified into any known functional domains.

In conclusion, Alg2 is a downstream mediator of Hivep3 in osteoblasts and chondrocytes. In addition to initiation of Runx2 protein degradation, Hivep3 interfered with the function of Runx2 via Alg2-mediated disturbance of localization and activity. In ATDC5 chondrocytes, Hivep3 and Alg2 enhanced mild ER stress to promote differentiation. Thus, our results are the first to link the ALG gene to differentiation of skeletal cells. Future studies on mice with knock-out of ALG genes, as well as detailed clinical research with corresponding CDG patients, may provide more information regarding the roles of ALG proteins in osteogenesis, chondrogenesis, and bone remodeling.

*Acknowledgments—The pEF-Shn3(Hivep3) expression vector was kindly provided by Dr. Laurie Glimcher. The mouse type II Runx2 expression plasmid and 6×OSE2 luciferase plasmid were kind gifts from Dr. Toshihisa Komori. The mutant 6×OSE2 luciferase plasmid was a kind gift from Dr. Gerard Karsenty. We gratefully acknowledge the technical assistance of Hui Gao.*

## REFERENCES

1. Kronenberg, H. M. (2003) Developmental regulation of the growth plate. *Nature* **423,** 332–336
2. Boyle, W. J., Simonet, W. S., and Lacey, D. L. (2003) Osteoclast differentiation and activation. *Nature* **423,** 337–342
3. Komori, T., Yagi, H., Nomura, S., Yamaguchi, A., Sasaki, K., Deguchi, K., Shimizu, Y., Bronson, R. T., Gao, Y. H., Inada, M., Sato, M., Okamoto, R., Kitamura, Y., Yoshiki, S., and Kishimoto, T. (1997) Targeted disruption of Cbfa1 results in a complete lack of bone formation owing to maturational arrest of osteoblasts. *Cell* **89,** 755–764
4. Mundlos, S., Otto, F., Mundlos, C., Mulliken, J. B., Aylsworth, A. S., Albright, S., Lindhout, D., Cole, W. G., Henn, W., Knoll, J. H., Owen, M. J., Mertelsmann, R., Zabel, B. U., and Olsen, B. R. (1997) Mutations involving the transcription factor CBFA1 cause cleidocranial dysplasia. *Cell* **89,** 773–779
5. Otto, F., Thornell, A. P., Crompton, T., Denzel, A., Gilmour, K. C., Rosewell, I. R., Stamp, G. W., Beddington, R. S., Mundlos, S., Olsen, B. R., Selby, P. B., and Owen, M. J. (1997) Cbfa1, a candidate gene for cleidocranial dysplasia syndrome, is essential for osteoblast differentiation and bone development. *Cell* **89,** 765–771
6. Gong, Y., Slee, R. B., Fukai, N., Rawadi, G., Roman-Roman, S., Reginato, A. M., Wang, H., Cundy, T., Glorieux, F. H., Lev, D., Zacharin, M., Oexle, K., Marcelino, J., Suwairi, W., Heeger, S., Sabatakos, G., Apte, S., Adkins, W. N., Allgrove, J., Arslan-Kirchner, M., Batch, J. A., Beighton, P., Black, G. C., Boles, R. G., Boon, L. M., Borrone, C., Brunner, H. G., Carle, G. F., Dallapiccola, B., De Paepe, A., Floege, B., Halfhide, M. L., Hall, B., Hennekam, R. C., Hirose, T., Jans, A., Jüppner, H., Kim, C. A., Keppler-Noreuil, K., Kohlschuetter, A., LaCombe, D., Lambert, M., Lemyre, E., Letteboer, T., Peltonen, L., Ramesar, R. S., Romanengo, M., Somer, H., Steichen-Gersdorf, E., Steinmann, B., Sullivan, B., Superti-Furga, A., Swoboda, W., van den Boogaard, M. J., Van Hul, W., Vikkula, M., Votruba, M., Zabel, B., Garcia, T., Baron, R., Olsen, B. R., and Warman, M. L. (2001) LDL receptor-related protein 5 (LRP5) affects bone accrual and eye development. *Cell* **107,** 513–523
7. Brunkow, M. E., Gardner, J. C., Van Ness, J., Paeper, B. W., Kovacevich, B. R., Proll, S., Skonier, J. E., Zhao, L., Sabo, P. J., Fu, Y., Alisch, R. S., Gillett, L., Colbert, T., Tacconi, P., Galas, D., Hamersma, H., Beighton, P., and Mulligan, J. (2001) Bone dysplasia sclerosteosis results from loss of the SOST gene product, a novel cystine knot-containing protein. *Am. J. Hum. Genet.* **68,** 577–589
8. Kato, M., Patel, M. S., Levasseur, R., Lobov, I., Chang, B. H., Glass, D. A., 2nd, Hartmann, C., Li, L., Hwang, T. H., Brayton, C. F., Lang, R. A., Karsenty, G., and Chan, L. (2002) Cbfa1-independent decrease in osteoblast proliferation, osteopenia, and persistent embryonic eye vascularization in mice deficient in Lrp5, a Wnt coreceptor. *J. Cell Biol.* **157,** 303–314
9. Li, X., Ominsky, M. S., Niu, Q. T., Sun, N., Daugherty, B., D'Agostin, D., Kurahara, C., Gao, Y., Cao, J., Gong, J., Asuncion, F., Barrero, M., Warmington, K., Dwyer, D., Stolina, M., Morony, S., Sarosi, I., Kostenuik, P. J., Lacey, D. L., Simonet, W. S., Ke, H. Z., and Paszty, C. (2008) Targeted deletion of the sclerostin gene in mice results in increased bone formation and bone strength. *J. Bone Miner. Res.* **23,** 860–869
10. Jones, D. C., Wein, M. N., Oukka, M., Hofstaetter, J. G., Glimcher, M. J., and Glimcher, L. H. (2006) Regulation of adult bone mass by the zinc finger adapter protein Schnurri-3. *Science* **312,** 1223–1227
11. Wu, L. C. (2002) ZAS: C2H2 zinc finger proteins involved in growth and development. *Gene Expr.* **10,** 137–152
12. Jin, W., Takagi, T., Kanesashi, S. N., Kurahashi, T., Nomura, T., Harada, J., and Ishii, S. (2006) Schnurri-2 controls BMP-dependent adipogenesis via interaction with Smad proteins. *Dev. Cell* **10,** 461–471
13. Shim, J. H., Greenblatt, M. B., Zou, W., Huang, Z., Wein, M. N., Brady, N., Hu, D., Charron, J., Brodkin, H. R., Petsko, G. A., Zaller, D., Zhai, B., Gygi, S., Glimcher, L. H., and Jones, D. C. (2013) Schnurri-3 regulates ERK downstream of WNT signaling in osteoblasts. *J. Clin. Invest.* **123,** 4010–4022
14. Wein, M. N., Jones, D. C., Shim, J. H., Aliprantis, A. O., Sulyanto, R., Lazarevic, V., Poliachik, S. L., Gross, T. S., and Glimcher, L. H. (2012) Control of bone resorption in mice by Schnurri-3. *Proc. Natl. Acad. Sci. U.S.A.* **109,** 8173–8178
15. Liu, S., Madiai, F., Hackshaw, K. V., Allen, C. E., Carl, J., Huschart, E., Karanfilov, C., Litsky, A., Hickey, C. J., Marcucci, G., Huja, S., Agarwal, S., Yu, J., Caligiuri, M. A., and Wu, L. C. (2011) The large zinc finger protein ZAS3 is a critical modulator of osteoclastogenesis. *PloS One* **6,** e17161
16. Saita, Y., Takagi, T., Kitahara, K., Usui, M., Miyazono, K., Ezura, Y., Na-

kashima, K., Kurosawa, H., Ishii, S., and Noda, M. (2007) Lack of Schnurri-2 expression associates with reduced bone remodeling and osteopenia. *J. Biol. Chem.* **282,** 12907–12915
17. Jones, D. C., Schweitzer, M. N., Wein, M., Sigrist, K., Takagi, T., Ishii, S., and Glimcher, L. H. (2010) Uncoupling of growth plate maturation and bone formation in mice lacking both Schnurri-2 and Schnurri-3. *Proc. Natl. Acad. Sci. U.S.A.* **107,** 8254–8258
18. Saito, A., Hino, S., Murakami, T., Kanemoto, S., Kondo, S., Saitoh, M., Nishimura, R., Yoneda, T., Furuichi, T., Ikegawa, S., Ikawa, M., Okabe, M., and Imaizumi, K. (2009) Regulation of endoplasmic reticulum stress response by a BBF2H7-mediated Sec23a pathway is essential for chondrogenesis. *Nat. Cell Biol.* **11,** 1197–1204
19. Bobick, B. E., and Kulyk, W. M. (2004) The MEK-ERK signaling pathway is a negative regulator of cartilage-specific gene expression in embryonic limb mesenchyme. *J. Biol. Chem.* **279,** 4588–4595
20. Tominaga, H., Maeda, S., Hayashi, M., Takeda, S., Akira, S., Komiya, S., Nakamura, T., Akiyama, H., and Imamura, T. (2008) CCAAT/enhancer-binding protein $\beta$ promotes osteoblast differentiation by enhancing Runx2 activity with ATF4. *Mol. Biol. Cell* **19,** 5373–5386
21. Alvarez, J., Sohn, P., Zeng, X., Doetschman, T., Robbins, D. J., and Serra, R. (2002) TGF$\beta$2 mediates the effects of hedgehog on hypertrophic differentiation and PTHrP expression. *Development* **129,** 1913–1924
22. Ducy, P., Starbuck, M., Priemel, M., Shen, J., Pinero, G., Geoffroy, V., Amling, M., and Karsenty, G. (1999) A Cbfa1-dependent genetic pathway controls bone formation beyond embryonic development. *Genes Dev.* **13,** 1025–1036
23. Geoffroy, V., Kneissel, M., Fournier, B., Boyde, A., and Matthias, P. (2002) High bone resorption in adult aging transgenic mice overexpressing cbfa1/runx2 in cells of the osteoblastic lineage. *Mol. Cell. Biol.* **22,** 6222–6233
24. Kelleher, D. J., and Gilmore, R. (2006) An evolving view of the eukaryotic oligosaccharyltransferase. *Glycobiology* **16,** 47R–62R
25. Thiel, C., Schwarz, M., Peng, J., Grzmil, M., Hasilik, M., Braulke, T., Kohlschütter, A., von Figura, K., Lehle, L., and Körner, C. (2003) A new type of congenital disorders of glycosylation (CDG-Ii) provides new insights into the early steps of dolichol-linked oligosaccharide biosynthesis. *J. Biol. Chem.* **278,** 22498–22505
26. Moremen, K. W., and Molinari, M. (2006) *N*-Linked glycan recognition and processing: The molecular basis of endoplasmic reticulum quality control. *Curr. Opin. Struct. Biol.* **16,** 592–599
27. Aebi, M., Bernasconi, R., Clerc, S., and Molinari, M. (2010) *N*-Glycan structures: Recognition and processing in the ER. *Trends Biochem. Sci.* **35,** 74–82
28. Yang, X., Matsuda, K., Bialek, P., Jacquot, S., Masuoka, H. C., Schinke, T., Li, L., Brancorsini, S., Sassone-Corsi, P., Townes, T. M., Hanauer, A., and Karsenty, G. (2004) ATF4 is a substrate of RSK2 and an essential regulator of osteoblast biology; implication for Coffin-Lowry syndrome. *Cell* **117,** 387–398
29. Murakami, T., Saito, A., Hino, S., Kondo, S., Kanemoto, S., Chihara, K., Sekiya, H., Tsumagari, K., Ochiai, K., Yoshinaga, K., Saitoh, M., Nishimura, R., Yoneda, T., Kou, I., Furuichi, T., Ikegawa, S., Ikawa, M., Okabe, M., Wanaka, A., and Imaizumi, K. (2009) Signalling mediated by the endoplasmic reticulum stress transducer OASIS is involved in bone formation. *Nat. Cell Biol.* **11,** 1205–1211
30. Saito, A., Ochiai, K., Kondo, S., Tsumagari, K., Murakami, T., Cavener, D. R., and Imaizumi, K. (2011) Endoplasmic reticulum stress response mediated by the PERK-eIF2$\alpha$-ATF4 pathway is involved in osteoblast differentiation induced by BMP2. *J. Biol. Chem.* **286,** 4809–4818
31. Korchynskyi, O., and ten Dijke, P. (2002) Identification and functional characterization of distinct critically important bone morphogenetic protein-specific response elements in the Id1 promoter. *J. Biol. Chem.* **277,** 4883–4891
32. Ishida, W., Hamamoto, T., Kusanagi, K., Yagi, K., Kawabata, M., Takehara, K., Sampath, T. K., Kato, M., and Miyazono, K. (2000) Smad6 is a Smad1/5-induced Smad inhibitor. Characterization of bone morphogenetic protein-responsive element in the mouse Smad6 promoter. *J. Biol. Chem.* **275,** 6075–6079
33. Garg, V., Muth, A. N., Ransom, J. F., Schluterman, M. K., Barnes, R., King, I. N., Grossfeld, P. D., and Srivastava, D. (2005) Mutations in NOTCH1 cause aortic valve disease. *Nature* **437,** 270–274
34. McLarren, K. W., Lo, R., Grbavec, D., Thirunavukkarasu, K., Karsenty, G., and Stifani, S. (2000) The mammalian basic helix loop helix protein HES-1 binds to and modulates the transactivating function of the runt-related factor Cbfa1. *J. Biol. Chem.* **275,** 530–538
35. Lee, J. S., Thomas, D. M., Gutierrez, G., Carty, S. A., Yanagawa, S., and Hinds, P. W. (2006) HES1 cooperates with pRb to activate RUNX2-dependent transcription. *J. Bone Miner. Res.* **21,** 921–933
36. Zaidi, S. K., Javed, A., Choi, J. Y., van Wijnen, A. J., Stein, J. L., Lian, J. B., and Stein, G. S. (2001) A specific targeting signal directs Runx2/Cbfa1 to subnuclear domains and contributes to transactivation of the osteocalcin gene. *J. Cell Sci.* **114,** 3093–3102
37. Kawamura, I., Maeda, S., Imamura, K., Setoguchi, T., Yokouchi, M., Ishidou, Y., and Komiya, S. (2012) SnoN suppresses maturation of chondrocytes by mediating signal cross-talk between transforming growth factor-$\beta$ and bone morphogenetic protein pathways. *J. Biol. Chem.* **287,** 29101–29113
38. Dai, H., Hogan, C., Gopalakrishnan, B., Torres-Vazquez, J., Nguyen, M., Park, S., Raftery, L. A., Warrior, R., and Arora, K. (2000) The zinc finger protein schnurri acts as a Smad partner in mediating the transcriptional response to decapentaplegic. *Dev. Biol.* **227,** 373–387
39. Udagawa, Y., Hanai, J., Tada, K., Grieder, N. C., Momoeda, M., Taketani, Y., Affolter, M., Kawabata, M., and Miyazono, K. (2000) Schnurri interacts with Mad in a Dpp-dependent manner. *Genes Cells* **5,** 359–369
40. Zheng, Q., Zhou, G., Morello, R., Chen, Y., Garcia-Rojas, X., and Lee, B. (2003) Type X collagen gene regulation by Runx2 contributes directly to its hypertrophic chondrocyte-specific expression *in vivo*. *J. Cell Biol.* **162,** 833–842
41. Haeuptle, M. A., and Hennet, T. (2009) Congenital disorders of glycosylation: an update on defects affecting the biosynthesis of dolichol-linked oligosaccharides. *Hum. Mutat.* **30,** 1628–1641
42. Coman, D., Irving, M., Kannu, P., Jaeken, J., and Savarirayan, R. (2008) The skeletal manifestations of the congenital disorders of glycosylation. *Clin. Genet.* **73,** 507–515
43. Asada, R., Kanemoto, S., Kondo, S., Saito, A., and Imaizumi, K. (2011) The signalling from endoplasmic reticulum-resident bZIP transcription factors involved in diverse cellular physiology. *J. Biochem.* **149,** 507–518


Cell Biology:

# Human Immunodeficiency Virus Type 1 Enhancer-binding Protein 3 Is Essential for the Expression of Asparagine-linked Glycosylation 2 in the Regulation of Osteoblast and Chondrocyte Differentiation

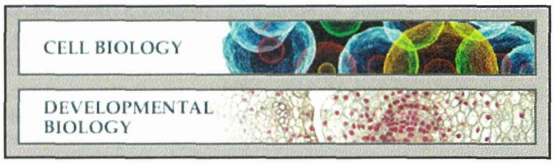


Katsuyuki Imamura, Shingo Maeda, Ichiro Kawamura, Kanehiro Matsuyama, Naohiro Shinohara, Yuhei Yahiro, Satoshi Nagano, Takao Setoguchi, Masahiro Yokouchi, Yasuhiro Ishidou and Setsuro Komiya

*J. Biol. Chem. 2014, 289:9865-9879.*
*doi: 10.1074/jbc.M113.520585 originally published online February 21, 2014*

---

THE JOURNAL OF BIOLOGICAL CHEMISTRY VOL. 289, NO. 12, pp. 8135–8150, March 21, 2014


# Bone Morphogenic Protein (BMP) Signaling Up-regulates Neutral Sphingomyelinase 2 to Suppress Chondrocyte Maturation via the Akt Protein Signaling Pathway as a Negative Feedback Mechanism*[S]

Received for publication, August 9, 2013, and in revised form, January 8, 2014 Published, JBC Papers in Press, February 6, 2014, DOI 10.1074/jbc.M113.509331

**Hironori Kakoi[‡1], Shingo Maeda[‡1,2], Naohiro Shinohara[‡§], Kanehiro Matsuyama[‡§], Katsuyuki Imamura[‡§], Ichiro Kawamura[§], Satoshi Nagano[§], Takao Setoguchi[¶], Masahiro Yokouchi[§], Yasuhiro Ishidou[‡], and Setsuro Komiya[‡§¶]**

*From the Departments of [‡]Medical Joint Materials and [§]Orthopaedic Surgery and [¶]Near-Future Locomotor Organ Medicine Creation Course, Graduate School of Medical and Dental Sciences, Kagoshima University, Kagoshima 890-8544, Japan*

**Background:** It is not clear how BMP-induced chondrocyte maturation is cell-autonomously terminated.
**Results:** BMP-2 induced the ceramide-generating enzyme neutral sphingomyelinase 2 (nSMase2) in chondrocytes, whereas silencing of nSMase2 enhanced maturation in an Akt signaling-dependent manner.
**Conclusion:** nSMase2 signaling regulates BMP-induced chondrocyte maturation as a negative feedback mechanism.
**Significance:** This study elucidated the novel link between BMP and lipid signaling in chondrogenesis.

**Although bone morphogenic protein (BMP) signaling promotes chondrogenesis, it is not clear whether BMP-induced chondrocyte maturation is cell-autonomously terminated. Loss of function of *Smpd3* in mice results in an increase in mature hypertrophic chondrocytes. Here, we report that in chondrocytes the Runx2-dependent expression of *Smpd3* was increased by BMP-2 stimulation. Neutral sphingomyelinase 2 (nSMase2), encoded by the *Smpd3* gene, was detected both in prehypertrophic and hypertrophic chondrocytes of mouse embryo bone cartilage. An siRNA for *Smpd3*, as well as the nSMase inhibitor GW4869, significantly enhanced BMP-2-induced differentiation and maturation of chondrocytes. Conversely, overexpression of *Smpd3* or $C_2$-ceramide, which mimics the function of nSMase2, inhibited chondrogenesis. Upon induction of *Smpd3* siRNA or GW4869, phosphorylation of both Akt and S6 proteins was increased. The accelerated chondrogenesis induced by *Smpd3* silencing was negated by application of the Akt inhibitor MK2206 or the mammalian target of rapamycin inhibitor rapamycin. Importantly, in mouse bone culture, GW4869 treatment significantly promoted BMP-2-induced hypertrophic maturation and calcification of chondrocytes, which subsequently was eliminated by $C_2$-ceramide. *Smpd3* knockdown decreased the apoptosis of terminally matured ATDC5 chondrocytes, probably as a result of decreased ceramide production. In addition, we found that expression of hyaluronan synthase 2 (*Has2*) was elevated by a loss of *Smpd3*, which was restored by MK2206. Indeed, expression of Has2 protein decreased in nSMase2-positive hypertrophic chondrocytes in the bones of mouse embryos. Our data suggest that the *Smpd3*/nSMase2-ceramide-Akt signaling axis negatively regulates BMP-induced chondrocyte maturation and Has2 expression to control the rate of endochondral ossification as a negative feedback mechanism.**

Over 95% of bone formation during the embryonic and developmental stages is achieved through endochondral ossification. This process is primed by the condensation of mesenchymal progenitor cells expressing the chondrogenic master regulator Sox9 (1), after which cells further differentiate into proliferating chondrocytes that are able to express a specific marker, *Col2a1*, encoding type II collagen (2). These chondrocytes then mature to hypertrophic chondrocytes, which eventually mineralize the surrounding cartilage matrix to be replaced by bone-forming osteoblasts (3). The maturation of chondrocytes into hypertrophic chondrocytes, which are able to express the type X collagen-encoding gene *Col10a1*, is mainly governed by the Runx2 transcription factor (4, 5). The rate of proliferation and differentiation of chondrocytes *in vivo* is tightly regulated by a signaling network between Indian hedgehog, parathyroid hormone-related protein, fibroblast growth factor (FGF), and bone morphogenetic protein (BMP)[3] signaling (6).

BMPs belong to the transforming growth factor-$\beta$ (TGF-$\beta$) family, which transduces signals through type II and type I receptors to activate receptor-regulated Smads. Upon ligand binding, BMP type I receptors phosphorylate Smad1/5/8 in the cytoplasm. Phosphorylated Smads form a trimeric complex

* This work was supported by Japan Society for the Promotion of Science KAKENHI Grants 25462376 (to H. K.), 23592221 (to S. M.), and 23592222 (to Y. I.), a grant from the Hip Joint Foundation of Japan (to S. M.), and a grant from the Cell Science Research Foundation (to S. M.).
[S] This article contains supplemental Table S1.
[1] Both authors contributed equally to this work.
[2] To whom correspondence should be addressed: Dept. of Medical Joint Materials, Graduate School of Medical and Dental Sciences, Kagoshima University, 8-35-1 Sakuragaoka, Kagoshima 890-8544, Japan. Tel.: 81-99-275-5381; Fax: 81-99-265-4699; E-mail: s-maeda@m3.kufm.kagoshima-u.ac.jp or maeda-s@umin.ac.jp.

[3] The abbreviations used are: BMP, bone morphogenic protein; nSMase2, neutral sphingomyelinase 2; MSC, mesenchymal stem/stroma cell; CHX, cycloheximide; RTK, receptor tyrosine kinase; OA, osteoarthritis; ITS, insulin/transferrin/selenium; PP2A, protein phosphatase 2A; rpS6, ribosomal protein S6.

with Smad4 (co-Smad) to translocate into the nucleus to directly or indirectly regulate the transcription of target genes (7, 8). BMPs and their receptors are expressed throughout the growth plate and perichondrium of developing bone (9). BMPs maintain expression of *Sox9* and subsequent cartilage matrix production (10, 11). BMPs are also required *in vitro* for the induction of *Col2a1* and *Col10a1* to promote chondrocyte maturation at later stages (12–14). Chondrocyte-specific overexpression of the extracellular BMP antagonist, Noggin, in transgenic mice resulted in no cartilage formation (15). Similarly, mice with cartilage-specific combined deletions of two BMP type I receptor genes (*Bmpr1a* and *Bmpr1b*), or with a double knock-out of *Smad1* and *Smad5*, showed severely impaired chondrogenesis (16, 17). At a later maturation stage, BMP signaling directly accelerates the expression of *Col10a1* in concert with Runx2 (13, 18, 19). Forced expression of constitutively active *Bmpr1a* in cartilage promoted the maturation and hypertrophy of chondrocytes in mice (20). The evidence clearly demonstrates the accelerating roles of BMP signaling in chondrocyte commitment, proliferation, and hypertrophic maturation both *in vivo* and *in vitro*.

Chondrogenesis in the endochondral ossification process is a promising cellular event for application in cartilage and bone regeneration, and it is a process that can be artificially engineered from human mesenchymal stem/stroma cells (MSCs) (21). Regarding the treatment of articular cartilage defects, the engineered chondrocytes must arrest maturation processes, because abnormally matured hypertrophic chondrocytes, expressing *COL10A1*, mineralize cartilage matrix to cause pathological conditions such as osteoarthritis (OA) (22–24). This is a major problem of cartilage tissue engineering in an *in vitro* culture system, where MSCs rapidly express *COL10A1* in a monolayer or pellet culture before the cells express hypertrophic phenotypes, suggesting that the mechanism by which MSCs induce type X collagen expression *in vitro* is different from that in chondrogenesis *in vivo* (25, 26). In bone engineering events, MSCs have formed bone trabeculae *in vivo* only when they had developed hypertrophic chondrocyte structure *in vitro* prior to implantation (21). Therefore, controlling the maturation and hypertrophy of chondrocytes is crucial for regenerative medicine of both cartilage and bone.

Although the effects of BMP signaling in promoting chondrocyte maturation should be eliminated for cartilage regeneration, they may be artificially enhanced to promote the efficiency of bone engineering. Although the BMP-Smad pathway directly induces the inhibitory Smad, Smad6, to inhibit the phosphorylation of Smad1/5/8 as a negative feedback mechanism (27), and Smurf1 targets Smad6 and the BMP type I receptors to block BMP signaling (28, 29), these inhibitory molecules are not specifically expressed in maturing chondrocytes. Recently, we reported that expression of the transcriptional repressor SnoN gradually increases in BMP-induced differentiating chondrocytes to suppress BMP signaling and the subsequent chondrocyte hypertrophic maturation (30). However, because SnoN partially blocked chondrocyte maturation, the mechanism regulating the rate of BMP signaling-driven chondrocyte differentiation in a cell-autonomous manner remains unclear.

The membrane-bound enzyme neutral sphingomyelinase 2 (nSMase2), encoded by the sphingomyelin phosphodiesterase 3 (*Smpd3*) gene, cleaves sphingomyelin to generate the lipid second messenger ceramide, which affects a variety of cellular process, including proliferation, apoptosis, and differentiation (31–34). A deletion mutation in the *Smpd3* gene was identified in fragilitas ossium (*fro*), a mouse model of osteogenesis imperfecta (35). *fro/fro* mice are characterized by retarded skeletal growth and a severely hypomineralized skeleton with normal osteoblast differentiation; bone mineralization can be rescued by osteoblast-specific overexpression of *Smpd3*, suggesting an important role of nSMase2 in the mineralization of the extracellular matrix (36). Interestingly, the number and area of hypertrophic chondrocytes were significantly increased, and conversion of cartilage into bone was retarded in *fro/fro* bone. *Smpd3* knock-out mice also showed fragile bones and dwarfism, with retarded transition of proliferative chondrocytes into hypertrophic chondrocytes (37, 38). Importantly, the knee joint cartilage of adult *Smpd3*-null mice showed severe deformity with exostosis, the phenotype of OA (38). These findings, from two lines of nSMase2 loss-of-function mice, suggest that *Smpd3*/nSMase2 plays an important role in suppressing hypertrophic maturation of chondrocytes and OA initiation. However, there is currently no information regarding the molecular mechanism for the function of nSMase2 in chondrocyte differentiation. In C2C12 myoblasts, BMP-2-induced Runx2 directly binds to the *Smpd3* promoter to up-regulate expression, suggesting that BMP signaling could elevate *Smpd3* level in a certain context (39).

In this study, we report that *Smpd3* is continuously up-regulated by BMP-2 stimulation of chondrocytes during the maturation stage to suppress the late differentiation step via the Akt pathway. We found that this induction of *Smpd3* by BMP-2 was Runx2-dependent and that the transcription factor is crucial for the hypertrophic maturation of chondrocytes. Loss- and gain-of-function experiments revealed that *Smpd3*/nSMase2 or ceramide signaling cell-autonomously suppressed expression of *Col2a1*, *Col10a1*, and hyaluronate synthase 2 (*Has2*), as well as accumulation of glycosaminoglycan. The Akt-S6 pathway was found to be responsible for the action of *Smpd3*/nSMase2. Importantly, application of an inhibitor compound for nSMase into the mouse bone organ culture system significantly increased the hypertrophic conversion and extracellular matrix calcification of cartilage.

## EXPERIMENTAL PROCEDURES

*Cell Culture and Differentiation*—The mouse chondrogenic cell line ATDC5, established from a differentiated culture of the teratocarcinoma stem cell line AT805 on the basis of chondrogenic potential (40), was obtained from the RIKEN BioResource Center. Human chondrocyte cell line C28/I2 was a kind gift from Dr. Mary Goldring (41). The cells were cultured in Dulbecco's modified Eagle's medium (DMEM)/Ham's F-12 (1:1) (Invitrogen), containing 5% fetal bovine serum (FBS) with 100 units/ml penicillin G and 100 μg/ml streptomycin. The mouse C3H10T1/2 cell line was obtained from the ATCC. The cells were cultured in Eagle's basal medium (Sigma) with 2 mM L-glutamine, 10% FBS, 100 units/ml penicillin G, and 100 μg/ml

streptomycin. Primary chondrocytes were harvested from 2-day-old mice with a C57BL/6J background. Briefly, articular cartilage of the femoral heads, femoral condyles, and tibial plateaus was isolated from mice and digested by 3 mg/ml collagenase D (Roche Applied Science) for 45 min, followed by 0.5 mg/ml collagenase D overnight. The chondrocytes were filtered through a sterile 40-$\mu$m cell strainer and cultured in DMEM/Ham's F-12 (1:1) containing 10% FBS, 100 units/ml penicillin G, and 100 $\mu$g/ml streptomycin. Differentiation of the cells, cultured in monolayer, was induced by the addition of recombinant human BMP-2 (PeproTech) at a concentration of 300 ng/ml, with or without insulin/transferrin/selenium (ITS) supplement (Sigma) on collagen type I-coated culture plates (Iwaki).

*Embryonic Bone Organ Culture*—Metatarsal bone rudiments were harvested from C57BL/6J mouse embryos at 16.5 days post-coitum (E16.5) and cultured in DMEM/Ham's F-12 (1:1) supplemented with 10% FBS, and 100 units/ml penicillin G, and 100 $\mu$g/ml streptomycin, as described (42). Cultured bones were stained with Alcian blue and alizarin red dyes according to a standard protocol for skeletal preparation. Briefly, bones fixed in 96% ethanol were stained with 0.015% Alcian blue 8GX (Sigma) in a mixture solution of 96% ethanol/acetic acid (4:1) for 1 day, followed by a dehydration step in 100% ethanol. Dehydrated bones were immersed briefly in 1% potassium hydroxide (KOH), followed by staining in 0.001% alizarin red S (Sigma) in 1% KOH for 1 day. Images were captured with stereomicroscope M165FC (Leica). Four bones per group were analyzed. Animal experiments were approved by the Institutional Animal Care and Use Committee of Kagoshima University (number MD12043).

*RNA Interference*—Dharmacon siRNA ON-TARGETplus SMARTpool, a mixture of four independent siRNAs against mouse *Runx1*, *Runx2*, *Runx3*, *Smpd3*, or *Has2*, and the control reagent were purchased from Thermo Scientific. siRNAs were transfected into cells using Lipofectamine RNAiMax (Invitrogen). BMP-2 and compounds were added to the culture simultaneously after an overnight transfection of siRNA.

*Plasmids and Adenovirus*—Mouse *Smpd3* cDNA was cloned from ATDC5 by employing an RT-PCR-based technique, subcloned into the entry vector, pENTR, and further transferred into the C-terminally V5-tagged expression vector, pEF-DEST51, by attL-attR recombination (Invitrogen). To generate adenovirus-carrying *Smpd3* cDNA, the *Smpd3* gene in the pENTR-Smpd3 vector was transferred into the C-terminally V5-tagged adenovirus expression vector pAd/CMV/V5-DEST by attL-attR recombination (Invitrogen) and further transfected into the adenovirus-producing cell line 293A according to the manufacturer's protocol. pAd/CMV/V5-GW/lacZ adenovirus expression vector was used as a control to express $\beta$-galactosidase. Adenovirus infection into ATDC5 cells was performed at a multiplicity of infection of 10. These experiments were approved by the Kagoshima University safety control committee for gene recombination techniques (number 22053).

*Chemical Inhibitor Compounds and $C_2$-ceramide*—All of the following agents were resolved in dimethyl sulfoxide (DMSO), and DMSO was used as the mock control. Cycloheximide was purchased from Sigma and applied at a concentration of 10 mM for 2 h, prior to BMP-2 stimulation. The nSMase inhibitor, GW4869 (Sigma), or $C_2$-ceramide (Enzo Life Sciences) was applied at the same time of BMP-2 induction, at 1 or 10 $\mu$M, respectively. The PI3K inhibitor, LY294002 (Sigma), Akt inhibitor, MK2206 (Chemie Tek), and the mammalian target of rapamycin inhibitor (Sigma) were applied at the same time of BMP-2 induction, at the indicated concentrations.

*Immunoblotting and RTK Signaling Antibody Array Analysis*—Cells were lysed in M-PER lysis buffer (Thermo Scientific) supplemented with aprotinin, sodium orthovanadate, and phenylmethylsulfonyl fluoride (PMSF) and subjected to SDS-PAGE, membrane transfer, and chemiluminescence, using standard protocol. Blots were incubated with the following: anti-Runx2 (1:1,000, 8G5, MBL); anti-nSMase2 (1:500, H-195, Santa Cruz Biotechnology); anti-aggrecan (1:500, H-300, Santa Cruz Biotechnology); anti-collagen type II $\alpha$1 (1:1,000, LSBio); anti-phospho-Akt (Ser-473) (1:1,000, 587F11, Cell Signaling); anti-Akt (1:1,000, 5G3, Cell Signaling); anti-phospho-S6 ribosomal protein (Ser-235/236) (1:1,000, D57.2.2E, Cell Signaling); anti-S6 ribosomal protein (1:1,000, 54D2, Cell Signaling); anti-phospho-PI3K (1:1,000, number 4228, Cell Signaling); anti-PI3K (p85) (1:1,000, number 610045, BD Transduction Laboratories); anti-phospho-Smad1/5/8 (1:1,000, number 9511, Cell Signaling); anti-Smad1 (1:1,000, number 9743, Cell Signaling); and horseradish peroxidase (HRP)-conjugated anti-rabbit secondary antibody, anti-mouse secondary antibody (1:10,000) (Cell Signaling), or anti-tubulin antibody (1:1,000, DM1A, T9026, Sigma). Signals were detected using the LAS 4000 Mini Image Analyzer (Fujifilm). We employed PathScan® RTK signaling antibody array kit (Cell Signaling) to analyze the signaling pathway influenced by loss of Smpd3/nSMase2 function. This system is a slide-based antibody array, founded upon the sandwich immunoassay principle and allowing for the simultaneous detection of 28 receptor tyrosine kinases and 11 important signaling nodes when phosphorylated at tyrosine or other residues, was employed to analyze the signaling pathway influenced by loss of *Smpd3*/nSMase2 function. The experiment was performed according to the manufacturer's manual, and the chemiluminescent readout was performed with LAS 4000 Mini Image Analyzer.

*Immunocytochemistry and Immunohistochemistry*—For immunocytochemistry, cells were fixed with 4% paraformaldehyde in PBS for 30 min and treated with 0.2% Triton X-100. CAS block (Zymed Laboratories Inc.) was used for blocking. For immunohistochemistry, formalin-fixed mouse E17.5 embryo humeri were embedded in paraffin blocks, which were sliced at a 4-$\mu$m thickness. The antigen was retrieved by the Liberate Antibody Binding solution (Polysciences). A CAS block was used for blocking. Cells or bone sections were incubated with anti-aggrecan (1:100, H-300, Santa Cruz Biotechnology), anti-collagen type II $\alpha$1 (1:100, LSBio), anti-nSMase2 rabbit polyclonal antibody (1:100, H-195, Santa Cruz Biotechnology), and anti-Has2 mouse monoclonal antibody (1:100, D-8, Santa Cruz Biotechnology). Anti-mouse Alexa Fluor 488 (1:200, A11001) or anti-rabbit Alexa Fluor 568 (1:200, A11011) (Invitrogen) was used to detect signals. Normal rabbit or mouse IgG was used as negative control. Hyaluronan (HA) detection

involved the following protocol. Samples were blocked with a streptavidin/biotin blocking kit (Vector Laboratories), according to the manufacturer's protocol, and digested sequentially with 0.05% of trypsin and 1 unit/ml of chondroitinase ABC (Sigma). Samples were further blocked with CAS block and sequentially incubated with biotin-conjugated HA-binding protein (1:1,000, Hokudo) and 1 μg/ml Alexa Fluor 488-conjugated streptavidin (Invitrogen). Images of immunocytochemistry and immunohistochemistry were captured with microscope AX80 and digital camera DP70 (Olympus). Animal experiments were approved by the Institutional Animal Care and Use Committee of Kagoshima University (number MD12043).

*Real Time Quantitative PCR Assay*—Cells were lysed with the TRIzol reagent (Invitrogen) to purify RNA, and 1 μg of RNA was reverse-transcribed into cDNA using the Verso cDNA kit (Thermo Scientific). The relative amount of gene transcripts was determined by real time PCR using the SYBR premix Ex TaqII (Takara) and the Thermal Cycler Dice TP850 (Takara). PCRs were performed in duplicate per sample, and the measured expression level of each gene was normalized to that of *Hprt1*. $\Delta C_t$ values were calculated by subtracting $C_t$ values of *Hprt1* from $C_t$ values of target genes. Sequence information of primers used is listed in supplemental Table 1.

*TUNEL Assay*—For detecting ATDC5 cells that underwent apoptosis, we used the ApopTag® peroxidase *in situ* apoptosis detection kit (Merck), which detects apoptotic cells *in situ* by labeling and detecting DNA strand breaks by the TUNEL method. The apoptotic cells were visualized by immunoperoxidase staining. Four independent experiments were performed, and four fields per well were evaluated for the number of apoptotic cells.

*Statistical Analysis*—Data in this study are expressed as mean ± S.D. of three independent experiments, unless otherwise noted. The statistical comparisons between the different treatments were performed using an unpaired Student's *t* test in which $p < 0.05$ was considered significant and $p < 0.01$ was highly significant.

## RESULTS

*Smpd3 Is Induced by BMP-2 in Chondrocytes and Is Detected in Mature Chondrocytes in Vivo*—We hypothesized that BMP signaling cell-autonomously activated unknown mechanisms to terminate BMP-induced chondrocyte differentiation through a negative feedback pathway. We focused on the *Smpd3* gene, because it could be up-regulated by BMP-2 in C2C12 myoblasts of mesenchymal origin (39); loss-of-function models for *Smpd3* in mice showed an increased number of hypertrophic chondrocytes or retarded transition of proliferative chondrocytes into hypertrophic chondrocytes. Molecular mechanisms for both cartilage phenotypes are unclear (37, 38), suggesting a relationship between BMP signaling and *Smpd3*/nSMase2 in chondrogenesis. To investigate the possible cell-autonomous roles of *Smpd3* in chondrocyte maturation, we mainly employed the clonal chondrogenic mouse cell line ATDC5 because it is an excellent *in vitro* model for skeletal development, which can be stimulated by BMP-2 (43, 44). We also used the normal human chondrocyte cell line C28/I2, mouse chondrogenic cell line C3H10T1/2, and mouse primary articular chondrocytes. We used BMP-2 to stimulate chondrogenic differentiation because, in addition to existing evidence, we and others have observed strong expression of the BMP-2 protein in proliferating and mature chondrocytes in the developing bones of rodents (45, 46). We first checked if these cell lines could differentiate into chondrocytes and mature into hypertrophic chondrocytes and not fibrochondrocytes. Upon BMP-2 induction, ATDC5 cells could produce chondrocyte-specific proteins, aggrecan and type II collagen, in the extracellular matrix (Fig. 1*A*). The early chondrocyte differentiation marker aggrecan (*Acan*) was elevated after day 1 and was maintained at elevated levels for 2 weeks, whereas *Col10a1* increased mildly from day 3 and was strongly up-regulated after day 7. *Col1a1* and *Col3a1* gene expression was not elevated, but rather decreased, suggesting that these cells did not differentiated into fibrochondrocytes (Fig. 1*B*). Similar results were obtained in C28/I2 cells (Fig. 1, *C* and *D*) and C3H10T1/2 cells (Fig. 1*E*). We also confirmed chondrogenic differentiation of primary chondrocytes by BMP-2 (Fig. 1*F*). $\Delta C_t$ values of quantitative PCR data indicated that primary chondrocytes express higher levels of chondrocyte marker genes than the three chondrogenic cell lines, suggesting that primary chondrocytes are already committed and differentiated into chondrocytes without BMP-2 induction, whereas the cell lines are relatively immature to differentiate into chondrocytes upon BMP stimulation. From these expression profiles, we considered these cell lines to be suitable models for chondrocyte differentiation. In ATDC5 cells, *Smpd3* showed a varied expression pattern from that of *Acan* and *Col10a1*, in that it was strongly elevated from day 1 and showed a second peak of increase after day 7 (Fig. 1*G*). We also observed the BMP-2-induced increment of the *Smpd3* gene in C28/I2, C3H10T1/2, and primary chondrocytes (Fig. 1*H*). Importantly, the primary chondrocytes also expressed higher levels of *Smpd3*, suggesting its functional importance in chondrocytes. If *Smpd3*/nSMase2 has an *in vivo* role in chondrogenesis or cartilage maintenance, it would be expressed in cartilage, although its expression in cartilage has not been characterized in detail. Quantitative PCR analysis on a panel of cDNAs from multiple tissues generated from 3-month-old mice revealed that *Smpd3* was expressed at the highest levels in the thymus, intestine, skin, fat, and bone, although it was almost absent in the heart, liver, and kidney (Fig. 1*I*). *Smpd3* was moderately expressed in cartilage tissue. This expression profile of *Smpd3* is essentially similar to the results reported for 2-week-old mice (36). In embryonic bone, we detected prominent expression of *Smpd3*-coding nSMase2 protein in the bone collar and trabecular bone by immunofluorescence (Fig. 1*J*). In the cartilage, little nSMase2 expression was noted in resting and columnar proliferating chondrocytes, whereas relatively high expression was observed in the prehypertrophic layer and hypertrophic chondrocytes (Fig. 1*J*), with an expression pattern resembling that of Runx2 (4).

*BMP-2-induced Increase of Smpd3 Expression Is Runx2-dependent*—We wondered if this BMP-2-induced expression of *Smpd3* in ATDC5 was directed by the BMP-Smad signaling axis, although the expression pattern was not the typical rapid pattern of a gene that is directly targeted (47). To test this, we treated ATDC5 cells with cycloheximide (CHX), an inhibitor of

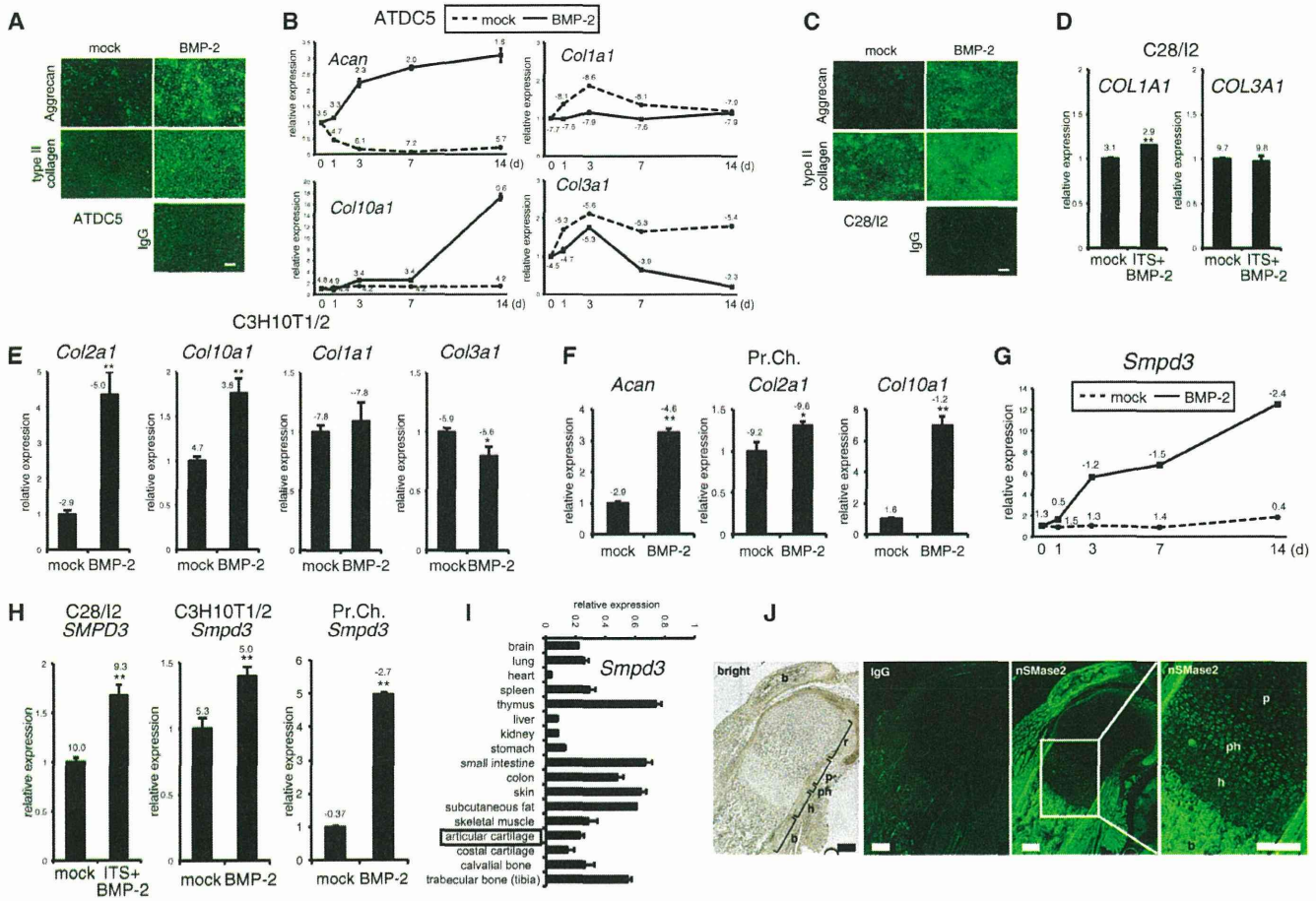


FIGURE 1. **Expression of *Smpd3*/nSMase2 is promoted by BMP-2 treatment in maturing chondrocytes *in vitro* and is increased in prehypertrophic and hypertrophic chondrocytes in a growth plate *in vivo*.** *A*, chondrogenic differentiation of mouse ATDC5 chondrocytes was induced by application of BMP-2 (300 ng/ml) for 7 days (*d*). Immunofluorescence for aggrecan or type II collagen was performed, with normal IgG as negative control. *Scale bar*, 100 $\mu$m. *B*, ATDC5 cells were cultured in the presence of BMP-2 (300 ng/ml) for the indicated periods. Expression levels of *Acan*, *Col10a1*, *Col1a1*, and *Col3a1* were examined by quantitative RT-PCR. *C*, chondrogenic differentiation of human C28/I2 chondrocytes was induced by the application of BMP-2 (300 ng/ml) for 7 days. Immunocytochemistry for aggrecan or type II collagen was performed, with normal IgG as negative control. *Scale bar*, 100 $\mu$m. *D*, C28/I2 chondrocytes were cultured in presence of BMP-2 (300 ng/ml) and ITS supplement for 14 days. Expression of *COL1A1* or *COL3A1* was evaluated by quantitative RT-PCR. *E*, mouse C3H10T1/2 cells were cultured with BMP-2 (300 ng/ml) for 48 h. Expression levels of *Col2a1*, *Col10a1*, *Col1a1*, and *Col3a1* were evaluated by quantitative RT-PCR. *F*, mouse primary chondrocytes (*Pr.Ch.*) cells were cultured in the presence of BMP-2 (300 ng/ml) for 6 days. Expression levels of *Acan*, *Col2a1*, and *Col10a1* were evaluated by quantitative RT-PCR. *G*, ATDC5 cells were cultured in presence of BMP-2 (300 ng/ml) for the indicated periods. Expression of *Smpd3* was examined by quantitative RT-PCR. *H*, quantitative RT-PCR for *Smpd3* was performed on samples in *D*, *E*, and *F*. *I*, real time PCR for *Smpd3* was performed on a tissue cDNA panel of a 3-month-old mouse. *J*, expression of nSMase2 in mouse E17.5 humerus cartilage was evaluated by immunofluorescence. Normal IgG was used as negative control. *r*, resting chondrocytes; *p*, proliferating chondrocytes; *ph*, prehypertrophic chondrocytes; *h*, hypertrophic chondrocytes; *b*, bone. *Scale bar*, 200 $\mu$m. *, $p < 0.05$; **, $p < 0.01$. $\Delta C_t$ values ($C_t$ target − $C_t$ Hprt1) of quantitative RT-PCR are indicated in the *graphs*.

*de novo* protein synthesis, before adding BMP-2. As expected, 24 h after BMP-2 stimulation, the induction of *Id1*, a representative direct-target gene of the BMP-Smad pathway, was maintained, even in the presence of CHX (Fig. 2*A*). Induction of *Id1* was higher in CHX-treated cells, likely because of the suppression of inhibitory Smad6 synthesis (27). However, expression of *Col2a1* was eliminated by CHX treatment (Fig. 1*A*). This basal suppression by CHX probably results from an inhibition of the constitutive expression of Sox9 and downstream Sox5 and Sox6, transcription factors that cooperatively activate the promoter of *Col2a1* (2, 48). However, existing Sox proteins should be responsible for the partially increased expression of *Col2a1* by BMP-2. The basal expression level of *Smpd3* was also suppressed by CHX treatment. Unlike *Col2a1*, however, the CHX-eliminated basal expression of *Smpd3* was not up-regulated by BMP-2 (Fig. 2*A*) suggesting that a *de novo* protein other than the Sox trio was necessary for BMP-induced expression of *Smpd3* in ATDC5 cells. Because the Runx2 protein is a master regulator of chondrocyte maturation (4, 5), and its direct interaction with the *Smpd3* promoter is important for its expression in myoblasts (39), we investigated the relationship between Runx2 and expression of *Smpd3* in chondrocytes. We confirmed the increment of the *Runx2* gene during BMP-induced maturation of ATDC5 chondrocytes (Fig. 2*B*). To address this question, we transfected ATDC5 cells with *Runx2* siRNA. At day 2 of BMP-2 application, *Runx2* was weakly induced, and its expression was knocked down by the siRNA to about 40% that of the control (Fig. 2*C*). Expression of *Id1* was not decreased by siRunx2, but rather it was increased, suggesting that Runx2 is inhibitory of the BMP pathway during this early differentiation stage. Interestingly, loss of Runx2 not only suppressed basal expression of *Smpd3* but also completely blocked induction by

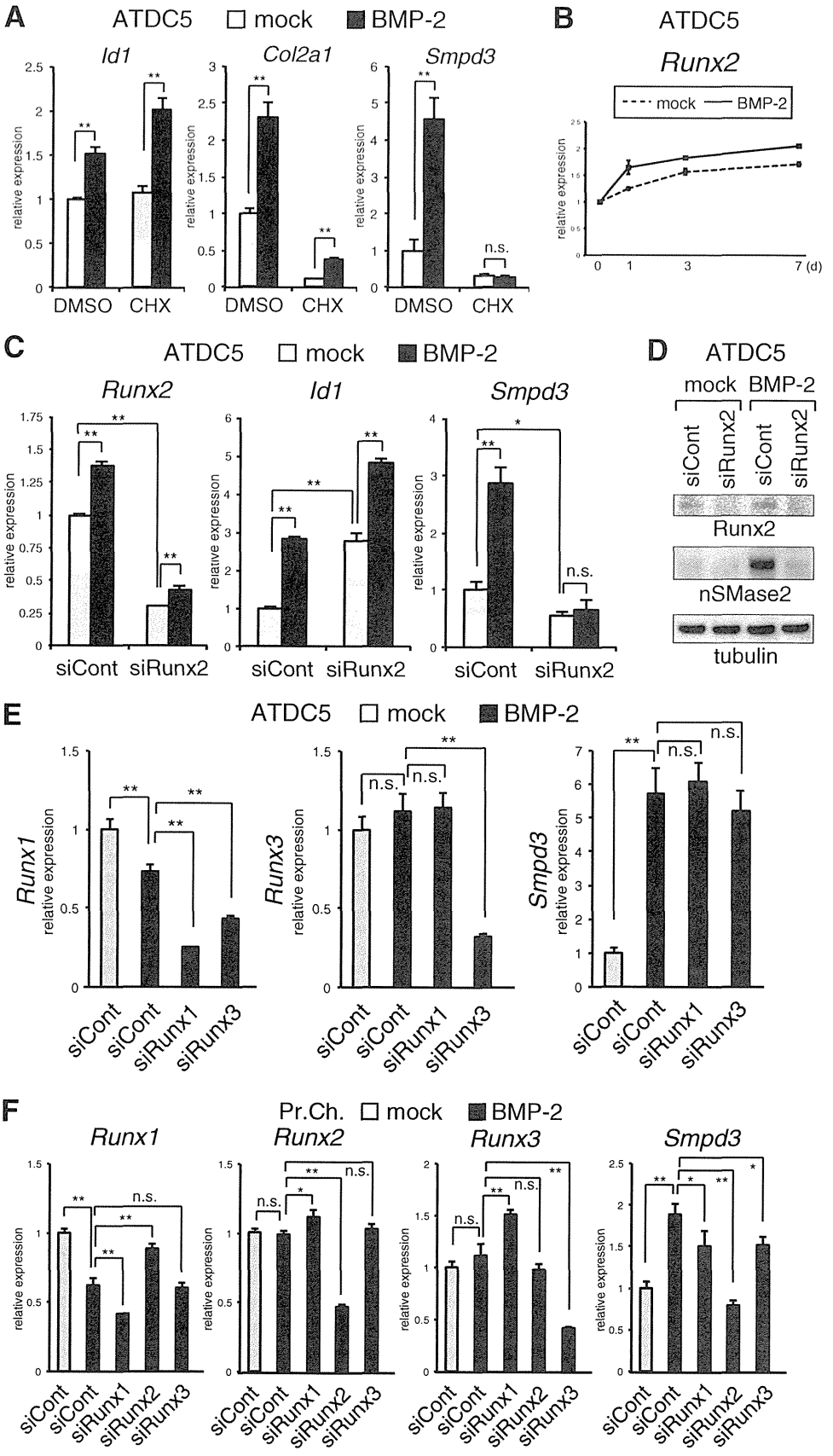
A
ATDC5
mock
BMP-2
Id1
Col2a1
Smpd3
relative expression
DMSO
CHX
B
ATDC5
Runx2
mock
BMP-2
relative expression
0
1
3
7 (d)
C
ATDC5
mock
BMP-2
Runx2
Id1
Smpd3
relative expression
siCont
siRunx2
n.s.
D
ATDC5
mock
BMP-2
siCont
siRunx2
siCont
siRunx2
Runx2
nSMase2
tubulin
E
ATDC5
mock
BMP-2
Runx1
Runx3
Smpd3
relative expression
n.s.
siCont
siCont
siRunx1
siRunx3
F
Pr.Ch.
mock
BMP-2
Runx1
Runx2
Runx3
Smpd3
relative expression
n.s.
siCont
siCont
siRunx1
siRunx2
siRunx3

BMP-2 treatment (Fig. 2*C*). This effect of siRunx2 was confirmed by analyzing protein expression of nSMase2 using immunoblotting (Fig. 2*D*). To assess the functional specificity of Runx2 among the three Runx isoforms, siRNAs for *Runx1* and *Runx3* were tested in ATDC5 cells. Although we could obtain efficient knockdown of *Runx1* and *Runx3*, the BMP-2-induced increase of *Smpd3* was not blocked by the corresponding siRNA (Fig. 2*E*). In primary chondrocytes, knockdown of *Runx2* completely abrogated the BMP-stimulated up-regulation of *Smpd3* (Fig. 2*F*). In contrast to ATDC5 cells, silencing of *Runx1* or *Runx3* could mildly suppress expression of *Smpd3* in primary chondrocytes (Fig. 2*F*), suggesting that Runx1 and Runx3 were partially responsible for *Smpd3* expression. These data demonstrate that BMP signaling increases the expression of *Smpd3*/nSMase2 in chondrocytes in cooperation with Runx2, especially in the maturation stages when the level of *Runx2* is elevated.

*Smpd3/nSMase2 and $C_2$-ceramide Inhibit Chondrogenic Differentiation and Maturation of Chondrocytes*—We used a knockdown assay to investigate whether *Smpd3*/nSMase2 has a role in the differentiation of ATDC5 chondrocytes. The potent induction of *Smpd3* by BMP treatment was silenced by siSmpd3 at a level of ~25% of that in cells treated with control siRNA at day 6 (Fig. 3*A*). Loss of *Smpd3* mildly increased the basal level of *Col2a1* expression and significantly enhanced the BMP-2-induced increment (Fig. 3*A*). Although expression of *Col10a1* was not significantly elevated by BMP-2 at day 6, it was dramatically increased by siSmpd3 in the presence of BMP-2. Similar effects of siSmpd3 on the expression of *Col2a1* and *Col10a1* were observed in primary chondrocytes (Fig. 5*F*). This effect of *Smpd3* knockdown against expression of *Col2a1* was mimicked by the addition of 1 $\mu$M GW4869, a specific inhibitor compound for nSMase (Fig. 3*B*) (49), suggesting that the data from the siSmpd3 experiment resulted from down-regulation of nSMase2. GW4869 also enhanced the production of the cartilage-specific extracellular component, glycosaminoglycan, by BMP-2 stimulation for 17 days, as assessed by Alcian blue staining, both in ATDC5 cells and in primary chondrocytes (Fig. 3*C*). Because nSMase2 generates ceramide as a lipid second messenger from the cell membrane, and the total level of ceramide was decreased in *fro/fro* bone (36), we challenged the cell membrane-permeable $C_2$-ceramide to mimic nSMase-ceramide signaling. Combined application of GW4869 and $C_2$-ceramide completely eliminated the GW4869-mediated enhancement observed by Alcian blue staining (Fig. 3*C*). The effect of GW4869 or $C_2$-ceramide on Alcian blue staining was confirmed by immunoblotting for aggrecan (Fig. 3*C*). Although $C_2$-ceramide showed no effect on BMP-2-induced expression of *Smpd3* at day 14, it significantly suppressed the expression of both *Col2a1* and *Col10a1* (Fig. 3*D*). As another gain-of-function approach, adenovirus-mediated overexpression of *Smpd3* in ATDC5 cells was performed to yield transgene expression levels that were ~100 times those of endogenous levels even after 8 days of induction (Fig. 3*E*). Infection of *Smpd3*-expressing adenovirus presented similar results as those of the $C_2$-ceramide experiment, in which overexpression inhibited the BMP-2-mediated elevation of both *Col2a1* and *Col10a1* expression (Fig. 3*E*). Similarly, Smpd3-expressing adenovirus suppressed maturation of primary chondrocytes (Fig. 3*F*). These loss- or gain-of-function experiments suggest a cell-autonomous inhibitory action of the *Smpd3*/nSMase2-ceramide axis on maturation of chondrocytes.

*Smpd3 Suppresses the Activity of the Akt-S6 Pathway during Chondrogenesis in Vitro*—We sought the molecular mechanism by which Smpd3/nSMase2 suppresses chondrogenesis and focused on the Akt signaling pathway for the following reasons. First, phosphorylation of Akt and the downstream ribosomal protein S6 (rpS6) was increased in *fro/fro* fibroblasts (50). Second, genetic approaches revealed that the IGF-IGF receptor-PI3K-Akt pathway plays key roles in skeletal growth and endochondral ossification and that overexpression of the activated form of Akt in the cartilage of transgenic mice promoted chondrocyte differentiation and maturation, whereas forced expression of its dominant-negative form delayed these cellular events (51). To evaluate the specificity of Akt among the various RTK signaling pathways, we examined the possible correlation of the Akt pathway in *Smpd3*/nSMase2 signaling during chondrocyte differentiation by performing an RTK signaling antibody array assay. Because receptors for insulin or insulin-like growth factor (IGF), which promote chondrogenic differentiation of ATDC5 cells (40), are RTKs, and a mixture of ITS is preferentially used to prepare the chondrogenic condition of ATDC5 cells (52), we first checked the effect of application of the ITS supplement alone and found no effect on the RTK array (Fig. 4*A*). Interestingly, 8 h after the addition of BMP-2, phosphorylation of rpS6 was significantly strengthened. More importantly, BMP-2-enhanced rpS6 phosphorylation was further increased by GW4869 or *Smpd3* knockdown, and these loss-of-function conditions for *Smpd3*/nSMase2 induced mild phosphorylation of Akt (Fig. 4*A*), suggesting that Akt and rpS6 are the specific targets of inhibition. This notion was further supported by an immunoblot assay using ATDC5 cells treated with siSmpd3 or Smpd3-expressing adenovirus. Application of BMP-2, in combination with the ITS supplement, dramatically induced expression of the nSMase2 protein, which was clearly diminished by transfecting with siRNA for *Smpd3* (Fig. 4*B*), even after 20 h of stimulation. Phosphorylation of Akt, as well as of rpS6, was significantly increased by

FIGURE 2. **BMP-2-induced increase of *Smpd3* expression in chondrocytes is Runx2-dependent.** *A*, CHX was applied to ATDC5 cells at a concentration of 10 mM for 2 h prior to BMP-2 (300 ng/ml) stimulation. Cells were harvested 24 h after BMP-2 induction to perform quantitative RT-PCR analysis for *Id1*, *Col2a1*, and *Smpd3*. *B*, ATDC5 cells were cultured with BMP-2 (300 ng/ml) for the indicated times. Expression of *Runx2* was examined by quantitative RT-PCR. *C*, ATDC5 chondrocytes were transfected with control siRNA (*siCont*) or *Runx2* siRNA (*siRunx2*) for 16 h and then treated with or without BMP-2 (300 ng/ml) for 48 h. Quantitative RT-PCR analysis was performed for *Runx2*, *Id1*, and *Smpd3*. *D*, ATDC5 cells were transfected with control siRNA (*siCont*) or *Runx2* siRNA (*siRunx2*) for 16 h and stimulated with BMP-2 (300 ng/ml) for 48 h. Cells were subjected to immunoblot analysis for the indicated antibodies. Tubulin served as a loading control. *E*, ATDC5 cells were transfected with control siRNA (*siCont*), *Runx1* siRNA (*siRunx1*), or *Runx3* siRNA (*siRunx3*) for 16 h and then treated with or without BMP-2 (300 ng/ml) for 48 h. Quantitative RT-PCR analysis was performed for *Runx1*, *Runx3*, and *Smpd3*. *F*, mouse primary chondrocytes were transfected with control siRNA (*siCont*), *Runx1* siRNA (*siRunx1*), *Runx2* siRNA (*siRunx2*), or *Runx3* siRNA (*siRunx3*) for 16 h and then treated with or without BMP-2 (300 ng/ml) for 48 h. Quantitative RT-PCR analysis was performed for *Runx1*, *Runx2*, *Runx3*, and *Smpd3*. *, $p < 0.05$; **, $p < 0.01$; *n.s.*, not significant.